

# Properties of conduction-band dilute-magnetic-semiconductor quantum wells in an in-plane magnetic field: A density of states profile that is not steplike

Constantinos Simserides

Leibniz Institute for Neurobiology, Special Lab for Non-Invasive Brain Imaging, Brenneckestrasse 6, D-39118 Magdeburg, Germany  
and Physics Department, Solid State Section, University of Athens, Panepistimiopolis, Zografos, GR-15784 Athens, Greece

(Received 6 September 2003; published 12 March 2004)

We examine how an in-plane magnetic field  $B$  modifies the density of states (DOS) in narrow-to-wide, conduction-band dilute-magnetic semiconductor quantum wells. We demonstrate that the DOS diverges significantly from the *ideal* steplike two-dimensional electron gas form and this causes severe changes to the physical properties, e.g., to the spin-subband populations, the internal and free energy, the Shannon entropy, and the in-plane magnetization  $M$ . We predict a considerable fluctuation of  $M$  in cases of vigorous competition between spatial and magnetic confinement.

DOI: 10.1103/PhysRevB.69.113302

PACS number(s): 73.20.-r, 85.75.-d, 75.75.+a, 65.40.Gr

When a magnetic field  $B$  is applied parallel to a quasi-two-dimensional electron gas (2DEG) layer, an interplay between spatial and magnetic localization is established. In the general case, it is necessary to compute self-consistently the energy dispersion.<sup>1,2</sup> In a dilute magnetic semiconductor (DMS) structure, due to the enhanced energy splitting between spin-up and spin-down states, all possible degrees of freedom become evident, and the density of states (DOS) acquires the form

$$n(\mathcal{E}) = \frac{A\sqrt{2m^*}}{4\pi^2\hbar} \sum_{i,\sigma} \int_{-\infty}^{+\infty} dk_x \frac{\Theta(\mathcal{E} - E_{i,\sigma}(k_x))}{\sqrt{\mathcal{E} - E_{i,\sigma}(k_x)}}. \quad (1)$$

The quasi-2DEG layer is parallel to the  $xy$  plane and  $B$  is applied along the  $y$  axis.  $\Theta$  is the step function,  $A$  is the  $xy$  area of the structure,  $m^*$  is the effective mass, and  $E_{i,\sigma}(k_x)$  are the spin-dependent  $xz$  plane eigenenergies which must be self-consistently calculated. Equation (1) is valid for any type of interplay between spatial and magnetic localization, i.e., for *narrow* as well as for *wide* quantum wells (QW's). In the limit  $B \rightarrow 0$ , the DOS retains the *famous* (and occasionally stereotypic) steplike 2DEG form. Another asymptotic limit of Eq. (1) is that of a simple saddle point, where the DOS diverges logarithmically.

Considerable advance has been achieved for III-V-based magnetic semiconductors which utilize the valence band<sup>3</sup> e.g., (In,Mn)As and (Ga,Mn)As. In view of that, we examine a system where conduction-band spintronics can be achieved; specifically we analyze n-doped *narrow-to-wide* DMS ZnSe/Zn<sub>1-x-y</sub>Cd<sub>x</sub>Mn<sub>y</sub>Se/ZnSe QW's. A principal reason which increases the influence of  $B$  and drives this system away from the parabolic dispersion is the relatively low conduction-band offset  $\Delta E_c$ . We use  $\Delta E_c = 1$  Hartree\*.<sup>4</sup> In the present system the *enhanced* electron spin-splitting  $U_{o\sigma}$  is not proportional to the cyclotron gap,  $\hbar\omega_c$ , i.e.,  $U_{o\sigma} = (g^*m^*/2m_e)\hbar\omega_c + N_0\eta\gamma(5/2)B_{5/2}(\xi) = \alpha + \beta$ .<sup>4</sup>  $g^*$  is the effective Landè factor and  $m_e$  is the electron mass. The term  $\beta$  arises from the exchange interaction between the conduction electron and the Mn<sup>+2</sup> cations.  $N_0$  is the concentration of cations and  $\eta$  is the expectation value of the exchange coupling integral over a unit cell.  $N_0\eta\gamma$  ( $\gamma = 0.035$ ) is taken

0.13 Hartree\*.<sup>4</sup>  $B_{5/2}(\xi)$  is the standard Brillouin function.  $\xi$  is a quantity with denominator  $k_B T$  and numerator containing two terms: the first one includes  $B$ , and the second one includes the difference between spin-up and spin-down populations.<sup>5,6</sup>  $T$  is the temperature and  $k_B$  is the Boltzmann constant. In the present paper  $T = 4.2$  K, thus  $B_{5/2}(\xi) \approx 1$ . Hence,  $\beta = 0.325$  Hartree\*. For ZnSe,  $\alpha \approx \tau 10^{-3}$  Hartree\*, where  $\tau$  is the arithmetic value of  $B$  in Tesla. The term  $\alpha$  is one or two orders of magnitude smaller than the term  $\beta$ . Therefore, it is convenient in the *first approximation* to ignore  $\alpha$ . For ZnSe, 1 Hartree\*  $\approx 70.5$  meV, thus  $\beta \approx 23$  meV. The electronic states' calculation and the material parameters can be found elsewhere.<sup>7,8</sup> Due to the numerical cost, the  $k_x$  dependence is often ignored.<sup>4,6</sup> However, this is adequate only if the spatial localization dominates.

The DOS is the *core* of the system and its changes affect all physical properties. If  $f_0(\mathcal{E})$  is the Fermi-Dirac distribution, the total electron population,  $N = \int_{-\infty}^{+\infty} d\mathcal{E} n(\mathcal{E}) f_0(\mathcal{E})$ , the internal energy,  $U = \int_{-\infty}^{+\infty} d\mathcal{E} n(\mathcal{E}) f_0(\mathcal{E}) \mathcal{E}$ , and the Shannon entropy,<sup>9</sup>  $S = -k_B \int_{-\infty}^{+\infty} d\mathcal{E} n(\mathcal{E}) f_0(\mathcal{E}) \ln[f_0(\mathcal{E})]$ . Hence,  $N$ ,  $U$ , and  $S$ , can be calculated.<sup>10</sup> Qualitatively, if  $N$  is kept constant, we expect that  $|U|$  will decrease whenever  $B$  induces flattening of the occupied spin-subbands, since this leads to occupied energies with smaller  $|\mathcal{E}|$ . On the other hand,  $S$  is sensitive to the changes of  $\ln[f_0(\mathcal{E})]$ . At  $T = 4.2$  K, these changes only occur in a short region around the chemical potential  $\mu \equiv 0$ . In other words,  $S$  reads the modification of the dispersion around  $\mu \equiv 0$ . The free energy  $F = U - TS$ . The main contribution to  $F$ —at this low  $T$ —comes from  $U$ . The in-plane magnetization,  $M = -(1/V)(\partial F/\partial B)_{N,T}$ , where  $V$  is the structure's volume. In the following, we deliberately keep  $T$  and  $N$  constant (we assume that all donors—e.g., Cl—are ionized).  $N/A = 1.566 \times 10^{11}$  cm<sup>-2</sup>. We symbolize 00 the ground-state spin-down-subband, 10 the first excited spin-down subband, 01 the ground-state spin-up subband, and finally 11 the first excited spin-up subband. To illustrate the antagonism between the spatial and the magnetic confinement we present results corresponding to different well widths  $L$ , i.e., 10 nm, 30 nm, and 60 nm. As a *unit* of DOS we use the ideal 2DEG step,  $(m^*A)/(\pi\hbar^2)$ .

For  $L = 10$  nm, the spatial confinement dominates. Even for  $B = 20$  T, the  $E_{i,\sigma}(k_x)$  retain a “parabolic shape” and the

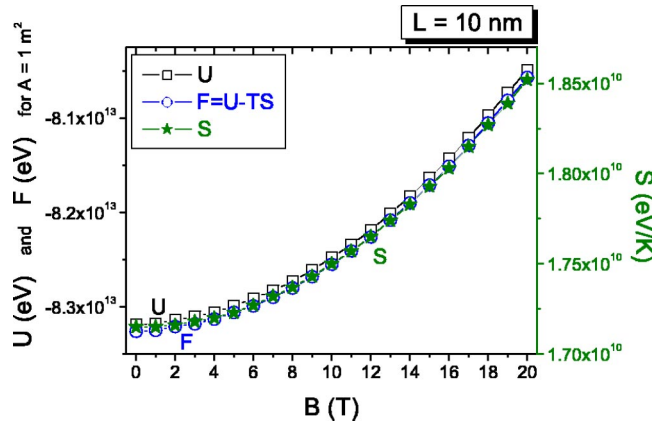


FIG. 1. (Color online)  $L=10$  nm. Internal energy  $U$ , free energy  $F$ , and entropy  $S$ , as a function of  $B$ . The dispersion is *almost parabolic* and increase of  $B$  induces a slight flattening of the spin subbands.

DOS is an almost “perfect staircase” with steps increasing  $\sim 7.5\%$  for the 00 spin subband and  $\sim 10\%$  for the 01 spin subband, relatively to the ideal 2DEG step. This increase is due to the  $B$ -induced slight flattening of the  $E_{i,\sigma}(k_x)$ . Only 00 is occupied. Figure 1 depicts  $U$ ,  $F$ , and  $S$  as a function of  $B$  in the range 0–20 T. All these physical properties exhibit “a single behavior” because the system has “almost parabolic” spin subbands.

Figures 2 and 3 demonstrate how the ideal picture is modified for  $L=30$  nm. Figure 2 presents the  $E_{i,\sigma}(k_x)$  and the DOS for characteristic values of  $B$ . Even for  $B=4$  T, since the  $E_{i,\sigma}(k_x)$  are no longer “perfect parabolas,” there is a quantitative modification of the DOS. For  $B=6$  T there are two impressive singularities and the DOS is quantitatively different from the ideal 2DEG staircase. Figure 3 depicts the spin-subband sheet electron populations,  $N_{ij}$ , as well as  $U$ ,  $F$ , and  $S$  as a function of  $B$  in the range 0–20 T. For  $B=0$  there are two populated spin subbands i.e.,  $N_{00}=1.397 \times 10^{11} \text{ cm}^{-2}$  and  $N_{10}=0.169 \times 10^{11} \text{ cm}^{-2}$ . In the region 0–6 T, we observe the gradual *depopulation* of the 10 spin subband. During this process, the perfect parabola is slightly distorted and the 10 partial DOS for  $B=6$  T looks like an “old abraded step.” In the region 4–12 T the 00 and 01 spin subbands change drastically, i.e., from almost parabolic with a single minimum gradually develop a two-minima shape. This is characteristically mirrored in the submersion of  $U$  and  $F$ . For  $B \geq 12$  T the dispersion retains the two-minima shape, while the basic effect of increasing  $B$  is the decrease of the electron concentration in the center of the well. As discussed above,  $S$  is very sensitive to these dispersion modifications.  $S$  clearly exhibits [Fig. 3(b)] “three distinct behaviors” approximately in the zones 0–4 T (concave down), 4–12 T (concave up), and 13–20 T (concave down). For the whole range 0–20 T,  $N$  is made up only from spin-down carriers. Even if some spin-up electrons survived, we could in principle utilize the effect of *depopulation* of the higher spin subbands to eliminate spin-up electrons.

Let us now consider a wider QW with  $L=60$  nm. For  $B=0$ , the partial DOS of all spin subbands is exactly 0.5 ideal 2DEG step. The 00–10 parabolas as well as the 01–11

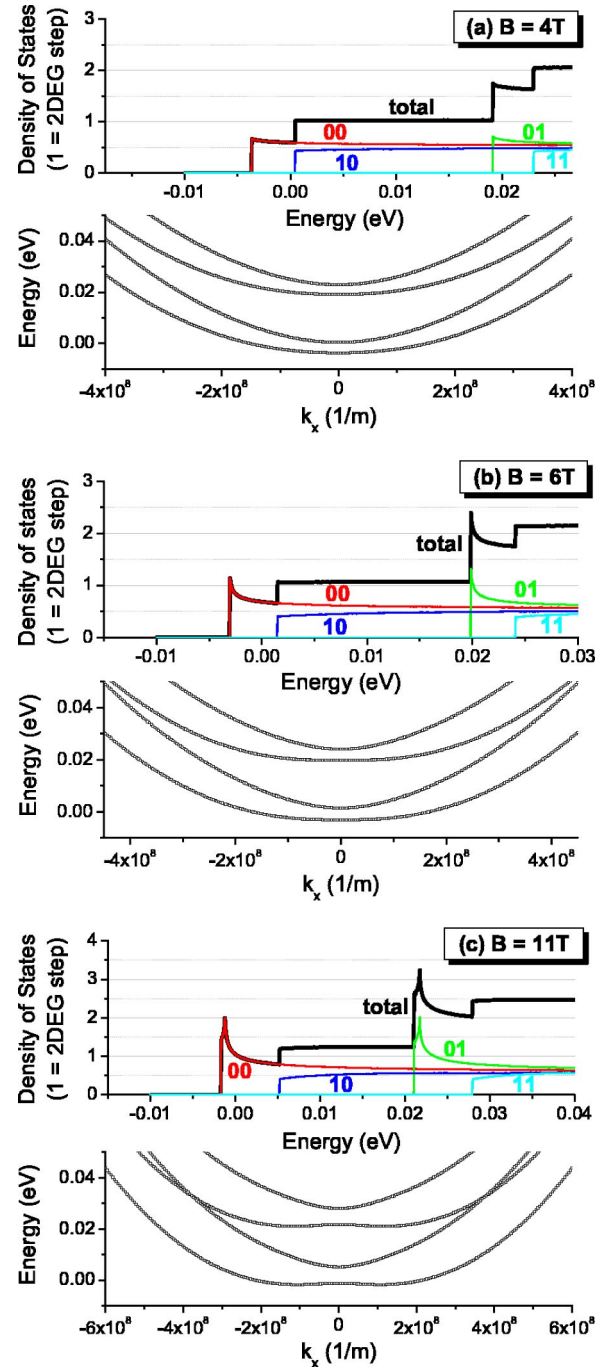


FIG. 2. (Color online)  $E_{i,\sigma}(k_x)$  and DOS for  $L=30$  nm. (a)  $B=4$  T, (b)  $B=6$  T, and (c)  $B=11$  T. In the region 4–12 T the 00 and 01 spin subbands change drastically, gradually developing a two-minima shape.

parabolas are energetically very close. The resulting populations are  $N_{00}=7.934 \times 10^{10} \text{ cm}^{-2}$ ,  $N_{10}=7.726 \times 10^{10} \text{ cm}^{-2}$ ,  $N_{01}=5.009 \times 10^{-15} \text{ cm}^{-2}$ , and  $N_{11}=4.316 \times 10^{-15} \text{ cm}^{-2}$ , i.e., only spin-down electrons survive. Only 10 has some population in the center of the well but the system is basically already a bilayer one. Figure 4 presents the  $E_{i,\sigma}(k_x)$  and the DOS for  $L=60$  nm and characteristic values of  $B$ . The ideal steplike DOS cannot describe the system even for relatively small  $B$ . For  $B=2$  T the two pairs of dispersion

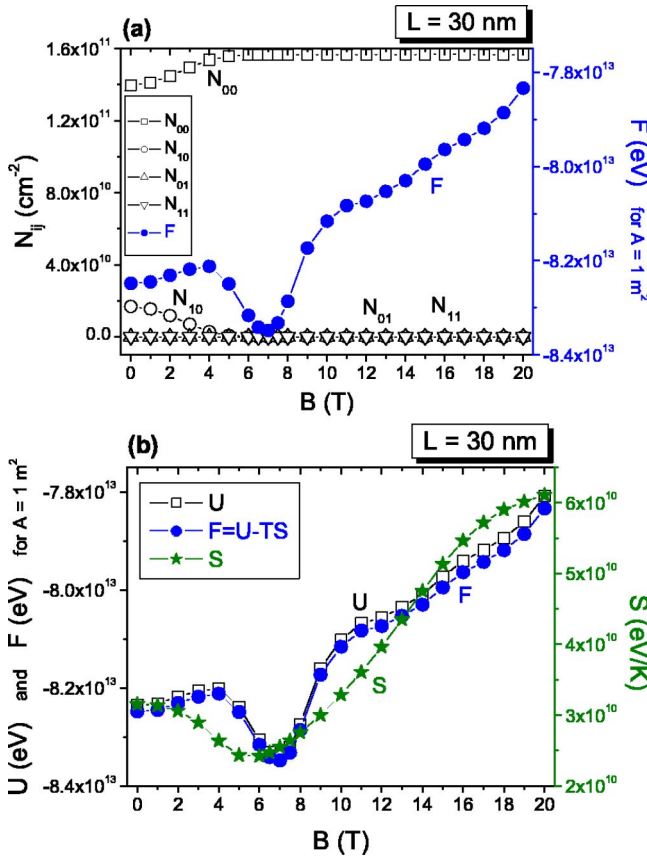


FIG. 3. (Color online)  $L = 30$  nm. (a) Spin-subband sheet electron populations  $N_{ij}$ , and free energy  $F$ ; (b) internal energy  $U$ , free energy  $F$ , and entropy  $S$ , as a function of  $B$ . The drastic dispersion modification is mirrored in the behavior of  $U$ ,  $F$ , and  $S$ .

curves corresponding to spin-down and spin-up electrons anticross at  $k_x = 0$  and the total DOS has been already slightly modified. For  $B = 7$  T some nice singularities are present while the shape and magnitude of the DOS is far away from the famous 2DEG staircase. For  $B = 20$  T the  $k_x = 0$  energy separation of the members of the spin-up and spin-down pairs is  $14.11$  meV  $\approx \hbar \omega_c = 14.47$  meV. Hence, in the center of the well the magnetic confinement has overcome the spatial confinement. In this region, the DOS is that of a free particle along the  $y$  axis plus a harmonic oscillator in the  $xz$  plane. Figure 5 presents  $N_{ij}$ , as well as  $U$ ,  $F$ , and  $S$ , as a function of  $B$  in the range  $0$ – $20$  T. Initially, in the zone  $0$ – $4$  T, the magnetic field depopulates the 10 spin subband. During this process the 10 dispersion retains a “one minimum” form. In the  $0$ – $4$  T range, the dispersion loses gradually the two-parabolas’ type, developing via anticrossing the two-minima shape in the 00 spin subband. In the  $4$ – $20$  T range, only the 00 spin subband remains populated retaining the two-minima shape. These two types of behavior can be seen in the modification of  $U$  and  $F$ . Again, more sensitive to these dispersion modifications is  $S$ , which is concave up in the  $0$ – $4$  T range but an absolutely straight line in the range  $4$ – $20$  T!

Using a derivative algorithm we obtain the in-plane magnetization (Fig. 6). Since  $L$  is different in these three cases, we present the product magnetization times volume  $MV$ , in

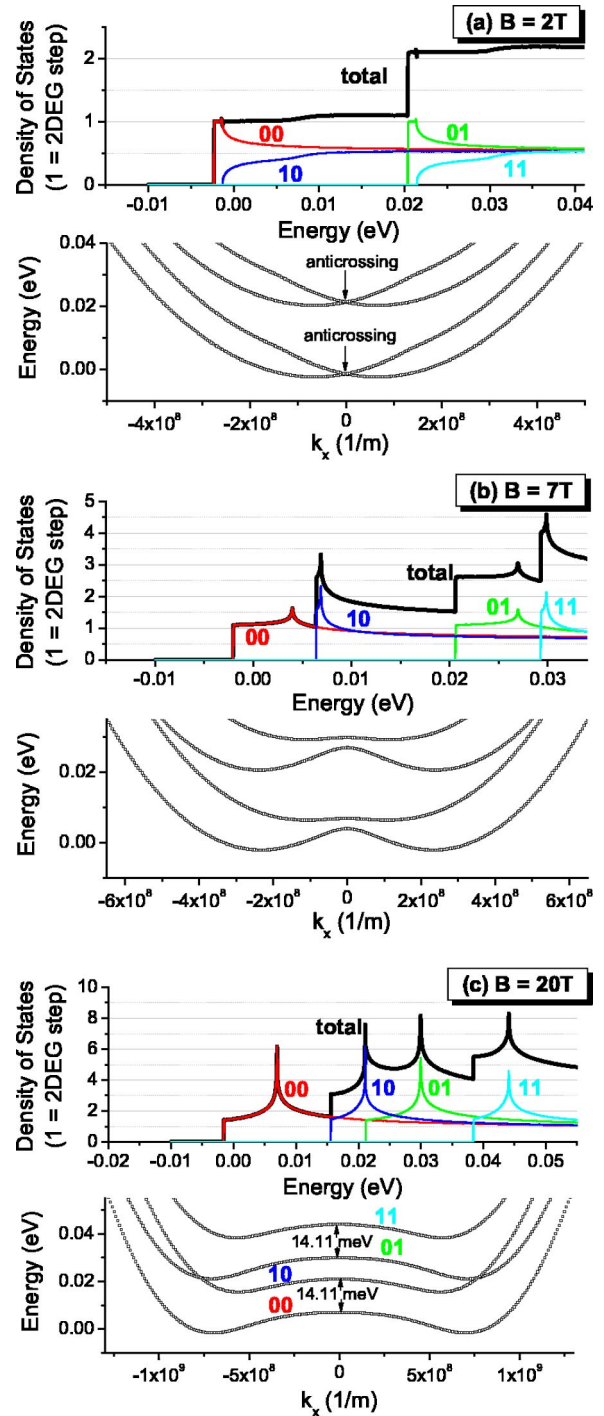


FIG. 4. (Color online)  $E_{i,c}(k_x)$  and DOS for  $L = 60$  nm. (a)  $B = 2$  T, (b)  $B = 7$  T, and (c)  $B = 20$  T. This is basically a spin-down bilayer system.

units of  $\text{eV/T}$  instead of  $M$  alone. For  $L = 10$  nm there is a simple almost straight line because the dispersion remains “basically parabolic.” For  $L = 60$  nm, since the structure “is basically a bilayer system” no big surprises are present. The situation is different for  $L = 30$  nm. Here, in the region where the dispersion changes drastically, we observe a severe fluctuation of  $M$ , which is so big that the lines for  $L = 10$  nm and  $L = 60$  nm seem almost constant. The magnitude of the magnetization fluctuation—for this 30 nm

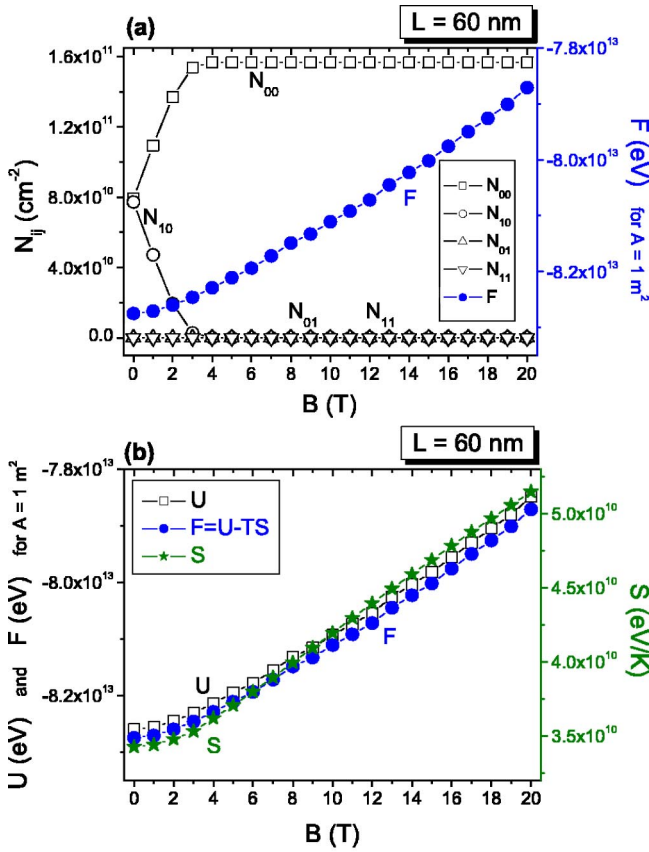


FIG. 5. (Color online)  $L = 60$  nm. (a) Spin-subband sheet electron populations  $N_{ij}$  and free energy  $F$ ; (b) internal energy  $U$ , free energy  $F$ , and entropy  $S$ , as a function of  $B$ . The two “dispersion zones,” 0–4 T and 4–20 T, are mirrored in the behavior of  $U$ ,  $F$ , and  $S$ .

well—is  $\approx 5 \text{ Am}^{-1}$ . This corresponds  $\sim$  to a Mn concentration of  $10^{17} \text{ cm}^{-3}$ . Conclusively, the DOS modification has caused an impressive effect on the system’s in-plane magnetization.

To our knowledge, there has been no experimental study of the present system under in-plane magnetic field. We note two photoluminescence studies performed in the Faraday geometry, with the magnetic field applied perpendicular to the

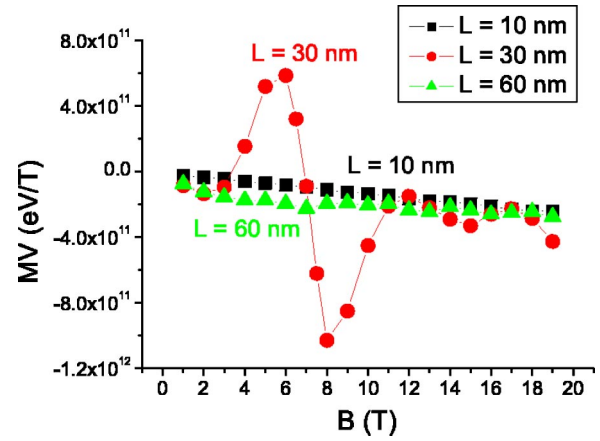


FIG. 6. (Color online) In-plane magnetization times volume  $MV$ , as a function of  $B$ . Note the fluctuation for  $L = 30$  nm due to the severe DOS modification.

layers: one of the narrow QW at 4.2 K (Ref. 11) and one of the asymmetric double QW at 1.8 K.<sup>12</sup> Interesting magnetic/nonmagnetic structures with different layers of ZnCdSe, ZnSe, and ZnCdMnSe have been magneto-optically investigated more recently,<sup>13,14</sup> without taking advantage of a parallel magnetic field. Hence, in order to exploit the potentialities of the present system we would like to encourage experiments with in-plane magnetic field and wider quantum wells.

We have illustrated—by providing results for different degrees of magnetic and spatial confinement—how much the *classical* staircase 2DEG density of states must be modified, for  $n$ -doped ZnSe/Zn<sub>1-x-y</sub>Cd<sub>x</sub>Mn<sub>y</sub>Se/ZnSe QW’s, under in-plane magnetic field. This is a valuable system for conduction-band spintronics. The DOS modification causes considerable effects on the system’s physical properties. We have described the changes induced to the spin-subband populations, the internal and free energy, the entropy, and the in-plane magnetization. We predict a significant fluctuation of the in-plane magnetization when the dispersion is severely modified by the parallel magnetic field.

I would like to thank Professor G. P. Triberis for general support, and Professor J. J. Quinn for correspondence and an older paper.

<sup>1</sup>C.D. Simserides, J. Phys.: Condens. Matter **11**, 5131 (1999).

<sup>2</sup>O.N. Makarovskii, L. Smrčka, P. Vašek, T. Jungwirth, M. Cukr, and L. Jansen, Phys. Rev. B **62**, 10 908 (2000).

<sup>3</sup>H. Ohno, J. Magn. Magn. Mater. **200**, 110 (1999); **242-245**, 105 (2002).

<sup>4</sup>S.P. Hong, K.S. Yi, and J.J. Quinn, Phys. Rev. B **61**, 13 745 (2000).

<sup>5</sup>B. Lee, T. Jungwirth, A.H. MacDonald, Phys. Rev. B **61**, 15 606 (2000).

<sup>6</sup>H.J. Kim and K.S. Yi, Phys. Rev. B **65**, 193310 (2002).

<sup>7</sup>C. Simserides, Physica E (Amsterdam) **21**, 956 (2004).

<sup>8</sup>H. Venghaus, Phys. Rev. B **19**, 3071 (1979); S. Adachi and T. Taguchi, *ibid.* **43**, 9569 (1991).

<sup>9</sup>C.E. Shannon, Bell Syst. Tech. J. **27**, 379 (1948).

<sup>10</sup> $N = \Gamma \sum_{i,\sigma} \int_{-\infty}^{+\infty} dk_x I$ ,  $S = -k_B \Gamma \sum_{i,\sigma} \int_{-\infty}^{+\infty} dk_x K$ ,  $U = \Gamma \sum_{i,\sigma} \int_{-\infty}^{+\infty} dk_x \times [E_{i,\sigma}(k_x) I + J]$ ,  $\Gamma = (A \sqrt{2m^*}) / (4\pi^2 \hbar)$ ,  $I = \int_0^{+\infty} (da / \sqrt{a}) \Pi$ ,  $J = \int_0^{+\infty} da \sqrt{a} \Pi$ ,  $K = \int_0^{+\infty} (da / \sqrt{a}) \Pi \ln \Pi$ ,  $\Pi = \{1 + \exp[(a + E_{i,\sigma}(k_x) - \mu) / k_B T]\}^{-1}$ .

<sup>11</sup>M.S. Salib, G. Kioseoglou, H.C. Chang, H. Luo, A. Petrou, M. Dobrowolska, J.K. Furdyna, and A. Twardowski, Phys. Rev. B **57**, 6278 (1998).

<sup>12</sup>W. Heimbrodt, L. Gridneva, M. Happ, N. Hoffmann, M. Rabe, and F. Henneberger, Phys. Rev. B **58**, 1162 (1998).

<sup>13</sup>M. Syed, G.L. Yang, J.K. Furdyna, M. Dobrowolska, S. Lee, and L.R. Ram-Mohan, Phys. Rev. B **66**, 075213 (2002).

<sup>14</sup>S. Lee, M. Dobrowolska, J.K. Furdyna, and L.R. Ram-Mohan, Phys. Rev. B **61**, 2120 (2000).